International Journal of Architectural, Civil and Construction Sciences
ISSN: 2415-1734
Vol:10, No:9, 2016

Study on Buckling and Yielding Behaviors of Low Yield Point Steel Plates

David Boyajian, Tadeh Zirakian

***Abstract*—**Stability and performance of steel plates are characterized by geometrical buckling and material yielding. In this paper, the geometrical buckling and material yielding behaviors of low yield point (LYP) steel plates are studied from the point of view of their application in steel plate shear wall (SPSW) systems. Use of LYP steel facilitates the design and application of web plates with improved buckling and energy absorption capacities in SPSW systems. LYP steel infill plates may yield first and then undergo inelastic buckling. Hence, accurate determination of the limiting plate thickness corresponding to simultaneous buckling and yielding can be effective in seismic design of such lateral force-resisting and energy dissipating systems. The limiting thicknesses of plates with different loading and support conditions are determined theoretically and verified through detailed numerical simulations. Effects of use of LYP steel and plate aspect ratio parameter on the limiting plate thickness are investigated as well. In addition, detailed studies are performed on determination of the limiting web-plate thickness in code-designed SPSWs. Some practical recommendations are accordingly provided for efficient seismic design of SPSW systems with LYP steel infill plates.

***Keywords*—**Plates, buckling, yielding, low yield point steel, steel plate shear walls.

I. Introduction

STABILITY and performance of steel plates are characterized by two independent phenomena, i.e. geometrical buckling and material yielding, which may interact with each other. Based on geometrical and material properties, material yielding may occur either before or after or even at the same time as buckling [1]. Accordingly, steel plates may be divided into slender, moderate, and stocky categories. Slender plates undergo elastic buckling and then yield in the post-buckling stage. Stocky plates, on the other hand, yield first and then undergo inelastic buckling, while moderate plates undergo simultaneous geometrical buckling and material yielding [2].

From the point of view of application in SPSW systems, thin and thick plates offer essentially disparate structural and economical characteristics. Thin plates are economically viable components; however, they possess relatively low buckling strength and weak energy absorption and serviceability characteristics. Thick plates, on the other hand, have comparatively higher buckling and energy dissipation capacities and improved serviceability characteristics, while economically are considered to be disadvantageous. Nowadays, use of LYP steel plates with extremely low yield strength and high ductility and elongation properties makes it possible to balance between structural and economical demands and consequently design SPSW systems with high buckling and energy dissipation capacities and also improved serviceability characteristics. LYP steel plates may undergo early material yielding followed by inelastic geometrical buckling. Such efficient lateral force-resisting and energy dissipating elements have been demonstrated [3], [4] to be quite favorable based on their superior characteristics and performance.

In order for efficient design and application of LYP steel plates, it is important to determine the limiting thickness corresponding to simultaneous geometrical buckling and material yielding. This can serve as an effective parameter in seismic design of SPSW systems with LYP steel infill plates as the primary lateral force-resisting and energy dissipating components. In this paper, the limiting thicknesses of LYP steel plates with various support and loading conditions are determined theoretically. The reliability of theoretical predictions is confirmed by numerical results. In addition, the advantages of use of LYP steel as compared to the conventional steel are demonstrated. Lastly, the limiting web-plate thicknesses in SPSW systems are determined and the accuracy of the results is verified via detailed numerical simulations.

II. Determination of Limiting Plate Thickness

Limiting thickness corresponds to concurrent geometrical buckling and material yielding of a steel plate. Concurrent geometrical-material bifurcation will occur when the plate's critical shear stress (τ_{cr}) is equal to its shear yield stress (τ_{yp}). Fig. 1 shows flat plates under pure shear, pure and uniform compression as well as combination of the two in-plane loadings, where l and h are the respective length and height of the plates.

The critical stress of rectangular plates under the action of shearing stresses uniformly distributed along the edges (Fig. 1 (a)) is given by $\tau_{cr} = \left[k_s \pi^2 E / 12(1-v^2)\right] \times \left(t_p / b\right)^2$. In addition, the critical stress of rectangular plates uniformly compressed in one direction (Fig. 1 (b)) is expressed by $\sigma_{cr} = \left[k_c \pi^2 E / 12(1-v^2)\right] \times \left(t_p / l\right)^2$. In these equations, E is Young's modulus, v is Poisson's ratio, and t_p is the plate

David Boyajian is with the Department of Civil Engineering and Construction Management, California State University, Northridge, CA, USA (e-mail: david.boyajian@csun.edu).

Tadeh Zirakian is with the Department of Civil Engineering and Construction Management, California State University, Northridge, CA, USA (Corresponding author; e-mail: tadeh.zirakian@csun.edu).

thickness. It is also noted that $a=\max(l,h)$ and $b=\min(l,h)$. k_s and k_c are buckling coefficients which can be determined from the figures and tables provided in stability books, e.g. [5]. Chen et al. [6] developed a concise formula, i.e. $\left(\sigma_{xx}/\sigma_{xx,cr}\right)^{\alpha}+\left(\sigma_{yy}/\sigma_{yy,cr}\right)^{\beta}+\left(\tau/\tau_{cr}\right)^{\gamma}=1.0$, for the critical buckling stresses of simply supported rectangular plates under combined biaxial compression and shear, as shown in Fig. 2. In this interaction equation, $\alpha=1$, $\gamma=2$, $\beta=1$ for $1\le a/b\le\sqrt{2}$, $\beta=(a/b)^{\left(1-(\tau/\tau_{cr})^2\right)}$ for $a/b>\sqrt{2}$, and $\sigma_{xx,cr}$, $\sigma_{yy,cr}$, and τ_{cr} are the respective critical stresses for pure compression in $x-$direction, pure compression in $y-$direction, and pure shear, which can be determined by using the classical equations.

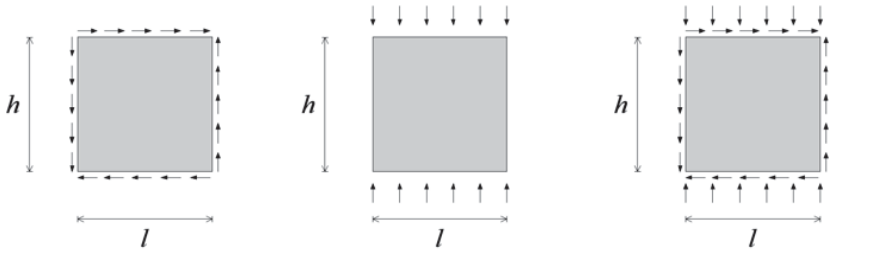

(a) Pure shear (b) Pure compression (c) Combined shear and compression

Fig. 1 Plates under shear and compressive loads

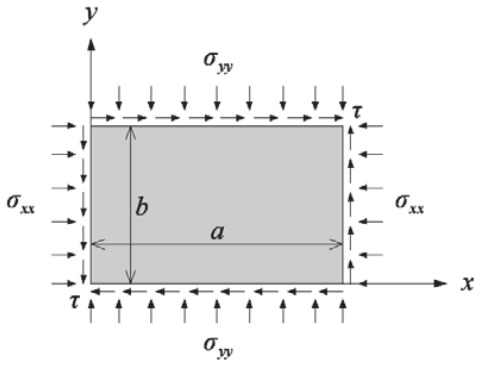

Fig. 2 Plate under combined shear and compressive loads [6]

The plate shear yield stress may be determined by considering the von Mises yield criterion, i.e. $(\sigma_{xx}-\sigma_{yy})^2+\sigma_{yy}^2+\sigma_{xx}^2+6\tau_{xy}^2=2\sigma_{yp}^2$. In this equation, σ_{xx}, σ_{yy}, and τ_{xy} are the in-plane normal and shear stresses, and also σ_{yp} is the plate yield stress. In order to obtain a general expression for the shear yield stress of a plate subjected to shear and uniaxial compressive loads representing the effects of lateral as well as vertical ground motion and/or gravity loads while used as a lateral force-resisting element in SPSW systems and as shown in Fig. 1 (c), it is assumed that $\sigma_{xx}=0$, $\sigma_{yy}=\sigma_c$, and $\tau_{xy}=\tau_{yp}$, where σ_c denotes the vertical uniformly-distributed compressive stress. As a result, τ_{yp} can be generally expressed as $\tau_{yp}=\sqrt{\left(\sigma_{yp}^2-\sigma_c^2\right)/3}$. In this study, two cases are considered as follows. First, plates are assumed to be subjected to pure shear, i.e. $\sigma_c=0$, which results in $\tau_{yp}=\sigma_{yp}/\sqrt{3}$. Second, plates are assumed to be subjected to combined shear and compressive loads, where compressive load is considered to be proportional and literally 50% of the shear load, i.e. $\sigma_c=0.5\tau_{yp}$, which in turn results in $\tau_{yp}=\sigma_{yp}/\sqrt{3.25}$. Lastly, in order to obtain the limiting thickness of a plate under pure shear, the critical shear stress (τ_{cr}) is set equal to $\sigma_{yp}/\sqrt{3}$, and for a plate subjected to combined shear and compressive loads τ in the interaction equation is substituted by $\sigma_{yp}/\sqrt{3.25}$. Characteristics of the considered LYP steel plates are summarized in Table I. E, v, and σ_{yp} are taken as 200 GPa, 0.3, and 100 MPa, respectively, in theoretical calculations.

III. Elastic Buckling Analysis and Verification of Results

The linear eigenbuckling analysis option of the finite element software, ANSYS 11.0 [7], is incorporated to determine the elastic critical loads of simply supported and clamped plates. Shell63 element is used for the linear/elastic buckling analysis. This four-node elastic element with six degrees of freedom at each node has both bending and membrane capabilities. Uniformly distributed shear and compressive loads are applied along the middle plane of the edge nodes, and the corner nodes are given half the value of the middle ones. In order to ensure high accuracy in modeling and analysis, convergence and mesh refinement studies are performed. As a result, 100×100 mm elements are taken as the minimum requirement in the analyses. The typical first buckling mode shapes of simply supported and clamped plates under pure shear, i.e. models P3 and P8, are shown in Fig. 3.

The theoretical and numerical predictions of elastic buckling loads of the plate models are tabulated in Table II. From the table, it is evident that the agreement between theoretical and numerical predictions is quite satisfactory and the discrepancy is below 5% in all cases.

TABLE I
CHARACTERISTICS OF PLATE MODELS

Model	$l \times h \times t_p$ (mm)	Load	Support	Type
P1	2000×3000×13.4	Pure Shear	Simple	Moderate
P2	3000×3000×11.7	Pure Shear	Simple	Slender
P3	3000×3000×17.5	Pure Shear	Simple	Moderate
P4	3000×3000×23.3	Pure Shear	Simple	Stocky
P5	4500×3000×20.1	Pure Shear	Simple	Moderate
P6	2000×3000×10.6	Pure Shear	Clamped	Moderate
P7	3000×3000×9.3	Pure Shear	Clamped	Slender
P8	3000×3000×14.0	Pure Shear	Clamped	Moderate
P9	3000×3000×18.7	Pure Shear	Clamped	Stocky
P10	4500×3000×15.8	Pure Shear	Clamped	Moderate
P11	2000×3000×15.8	Shear & Comp.	Simple	Moderate
P12	3000×3000×15.1	Shear & Comp.	Simple	Slender
P13	3000×3000×22.7	Shear & Comp.	Simple	Moderate
P14	3000×3000×30.3	Shear & Comp.	Simple	Stocky
P15	4500×3000×28.4	Shear & Comp.	Simple	Moderate
P16	2000×3000×12.2	Shear & Comp.	Clamped	Moderate
P17	3000×3000×10.9	Shear & Comp.	Clamped	Slender
P18	3000×3000×16.4	Shear & Comp.	Clamped	Moderate
P19	3000×3000×21.9	Shear & Comp.	Clamped	Stocky
P20	4500×3000×19.5	Shear & Comp.	Clamped	Moderate

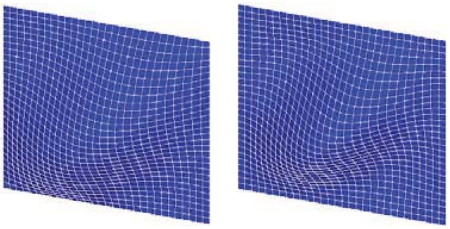

(a) Model P3 **(b)** Model P8

Fig. 3 Typical first buckling mode shapes

IV. BUCKLING AND YIELDING BEHAVIOR OF STEEL PLATES

The nonlinear large deflection static analysis of ANSYS 11.0 [7] is used for nonlinear buckling analysis of plates. Shell181 element is used for nonlinear analysis. This four-node element with six degrees of freedom at each node is suitable for analyzing thin to moderately-thick shell structures and is also well-suited for linear, large rotation, and/or large strain nonlinear applications.

LYP100 steel with a bilinear material stress-strain relationship is adopted for nonlinear buckling analyses. Material properties are consistent with those applied in theoretical calculations as mentioned in Section II, and the tangent modulus (E_t) is taken as 3333.3 MPa. Moreover, the von Mises yield criterion is used for material yielding, and the isotropic hardening rule is also incorporated in the nonlinear pushover analyses.

In order to initiate buckling, a very small out-of-plane force of about 0.01% of the plate elastic buckling capacity is applied at the center of the plate, which is also consistent with the first buckling mode shape of the plate.

TABLE II
THEORETICAL AND NUMERICAL ELASTIC BUCKLING LOADS OF PLATES

Model	$P_{cr-Theoretical} = \tau_{cr} \times lt_p$ (kN)	$P_{cr-Numerical}$ (kN)	Discrepancy (%)
P1	1550.05	1532.98	1.1
P2	902.31	898.05	0.5
P3	3019.34	3005.10	0.5
P4	7126.32	7092.60	0.5
P5	5231.42	5182.20	0.9
P6	1234.57	1227.02	0.6
P7	706.63	707.19	0.1
P8	2410.61	2412.54	0.1
P9	5744.71	5749.20	0.1
P10	4088.55	4075.11	0.3
P11	1753.19	1718.84	2.0
P12	1112.12	1097.58	1.3
P13	3779.55	3729.00	1.3
P14	8990.01	8868.30	1.4
P15	7076.59	6772.95	4.3
P16	1354.91	1337.30	1.3
P17	799.52	768.24	3.9
P18	2723.22	2616.72	3.9
P19	6484.59	6231.00	3.9
P20	4855.01	4681.80	3.6

The geometrical as well as material nonlinearities of plates are included in the analyses, and the arc-length method is implemented to achieve a fast convergence and capture the unloading behavior of the plate. The typical buckling and yielding behaviors of slender, moderate, and stocky plates, obtained from the nonlinear buckling analyses are shown in Fig. 4.

From Fig. 4, it is evident that slender plates experience elastic buckling and continue to absorb more load beyond their buckling capacity up to the ultimate load which is in turn followed by softening. Moderate plates with the theoretically-predicted limiting thicknesses, on the other hand, undergo simultaneous buckling and yielding which is followed by sudden stiffness loss, while the stocky plates yield first and then undergo post-yield plastic buckling which is considerably below their elastic critical loads. In addition, it is clearly observed that slender plates possess post-buckling reserve, and the stocky plates exhibit some post-yield strength, whereas the moderate plates exhibit neither post-buckling nor post-yield reserves. Slender plate models P2, P7, P12, and P17 possess 26%, 29%, 24%, and 28% post-buckling reserve, respectively, which indicates that consideration of the compressive load slightly reduces the post-buckling reserve. On the other hand, stocky plate models P4, P9, P14, and P19 possess 1%, 2%, 10%, and 12% post-yield reserve, respectively, which demonstrates that consideration of the compressive load results in considerable increase in post-yield reserve.

Lastly, results of the nonlinear buckling analyses indicate that limiting plate thickness is accurately predicted theoretically in all considered cases.

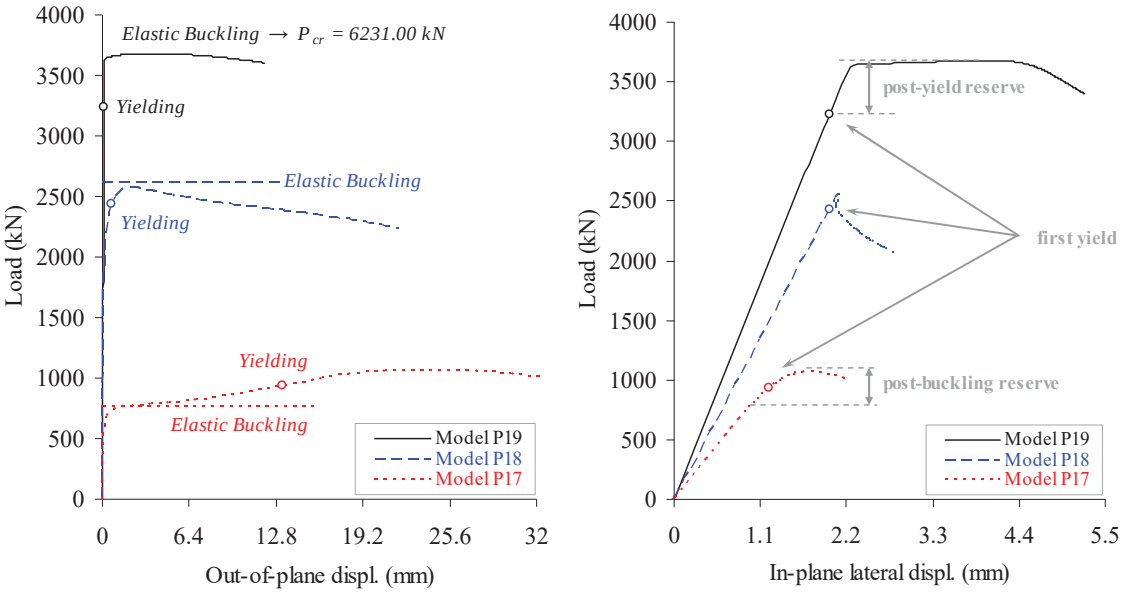

(a) Load vs. out-of-plane displ. curves (b) Load vs. in-plane lateral displ. curves

Fig. 4 Typical buckling and yielding behaviors of steel plates

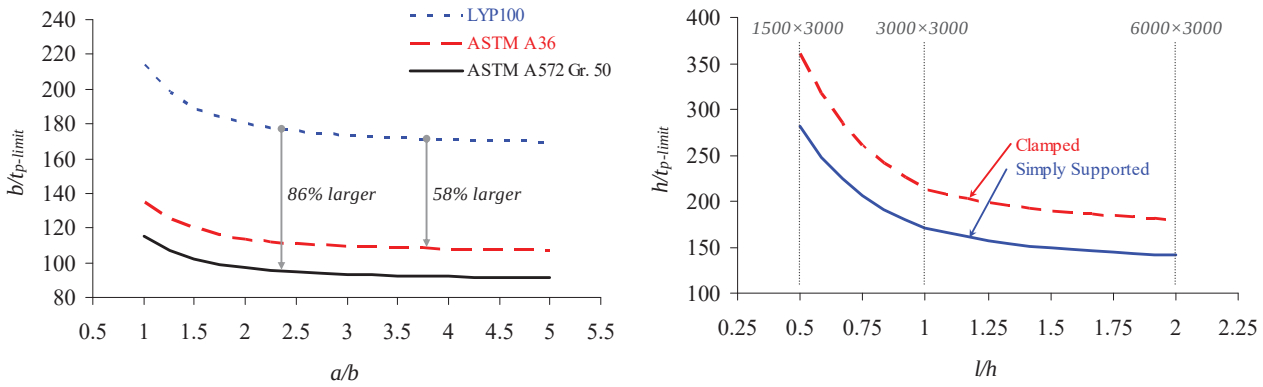

(a) Use of LYP steel (clamped plate) (b) Plate aspect ratio

Fig. 5 Effects of material and geometrical parameters on limiting plate thickness

V. Effects of Material and Geometrical Parameters on Limiting Plate Thickness

The limiting thickness of a plate is a function of its material and geometrical properties. In this section, the effects of use of LYP steel material and plate aspect ratio on the limiting plate thickness are investigated.

ASTM A36 steel with σ_y = 250 MPa is generally the preferred material standard for plates. ASTM A572 Gr. 50 steel with σ_y = 345 MPa, on the other hand, is quite common for structural components with plates thicker than 3/4 in or 19.05 mm [8]. LYP100 steel with $\sigma_y \approx$ 100 MPa has also been developed by Nippon Steel Corporation in Japan as a result of studies on seismic control structures with high energy absorption capacity [9]. The advantages of use of LYP100 steel in lowering the limiting plate thickness are demonstrated in Fig. 5 (a). In the figure, $b/t_{p-limit}$ slenderness ratios for clamped plates are plotted against a broad range of a/b aspect ratios for the three steel material types, where $t_{p-limit}$ is the limiting plate thickness. It is observed that application of LYP100 steel results in 58% and 86% larger $b/t_{p-limit}$ slenderness ratios relative to the application of ASTM A36 and ASTM A572 Gr. 50 steel material, respectively. Larger $b/t_{p-limit}$ slenderness ratio implies smaller limiting plate thickness required to impose the concurrent geometrical-material bifurcation condition. Consistent results are obtained for plates with simple supports. It is concluded that use of LYP100 steel substantially reduces the limiting plate thickness compared to the conventional steel material. This indicates that seismic performance of SPSW systems in general, and energy absorption capacity of the infill plates in particular can

be improved by using LYP steel in lieu of employing thick and/or heavily-stiffened conventional steel web-plates.

The effects of aspect ratio on the limiting thicknesses of simply supported and clamped plates are also demonstrated in Fig. 5 (b), in which $h/t_{p-limit}$ slenderness ratios determined by considering LYP100 steel material are plotted against l/h aspect ratios. As illustrated in the figure, this case study covers practical ranges of plate dimensions as well as aspect ratios. From the figure, it is evident that $h/t_{p-limit}$ ratio generally decreases in both support condition cases as l/h ratio increases. However, it is observed that rate of change of $h/t_{p-limit}$ ratios in both cases is high for l/h ratios between 0.5 and 1.0. In other words, limiting plate thickness reduces as the plate length-to-height ratio decreases and this reduction is further pronounced as the aforementioned aspect ratio becomes smaller than 1.0. This issue is of practical importance in design of SPSWs with high energy absorption capacity, since wider infilled spans in buildings will require thicker plates to provide high seismic performance, which may be uneconomical.

VI. Determination of Limiting Plate Thickness in Steel Shear Wall Systems

This section focuses on determination of the limiting plate thickness in SPSWs where infill plates are surrounded by horizontal and vertical boundary elements, i.e. HBEs and VBEs. Nonlinear finite element analysis is performed on five code-designed SPSWs (Table III) to learn about the real amount of fixity of the edge supports of infill plates in steel shear wall systems. The web plate dimensions are consistent with those of models P6 through P10 in Table I, and the frame members are designed based on the AISC 341-10 [10] code requirements.

TABLE III
Characteristics of Code-Designed SPSW Models

Model	Web plate $l \times h \times t_p$ (mm)	HBE (beam)	VBE (column)
SPSW1	2000×3000×10.6	W14×120	W14×311
SPSW2	3000×3000×9.3	W14×233	W14×257
SPSW3	3000×3000×14.0	W14×311	W14×342
SPSW4	3000×3000×18.7	W14×398	W14×426
SPSW5	4500×3000×15.8	W30×391	W14×370

Finite element models of the SPSWs with geometrical and material nonlinearities are developed and analyzed by using ANSYS 11.0 [7] software. Shell181 element is used to model the infill plate and boundary frame members. The columns are fully fixed at their bases and the exterior nodes of the column flange and stiffener elements around the perimeter of the panel zones are restrained against out-of-plane displacement. Very small initial out-of-plane deformations of about $\sqrt{l \times h}/1000$ and proportional to the lowest eigen-mode shape of elastic buckling are introduced to the plates. LYP100 and ASTM A572 Gr. 50 steel materials (Fig. 6) are used for the web plate and frame members, respectively. Furthermore, the von Mises yield criterion is used for material yielding, and the isotropic and kinematic hardening rules are incorporated in the respective nonlinear pushover and cyclic analyses. In-plane lateral load is applied to the beam-column connection in a displacement-controlled and incremental manner. Numerical modeling of SPSWs is validated by considering the experimental results of specimen no. 1 tested by [3]. As shown in Fig. 7, agreement between the experimental and numerical results is quite satisfactory. The finite element models and first buckling mode shapes of SPSWs with different aspect ratios and geometrical properties are shown in Fig. 8.

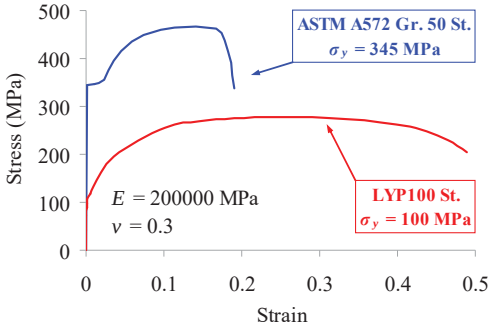

Fig. 6 Steel material properties

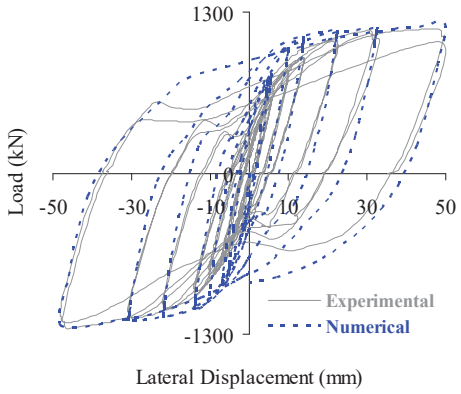

Fig. 7 Validation of SPSW modeling

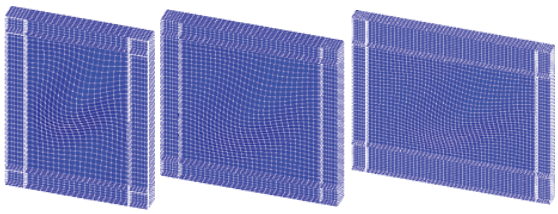

(a) SPSW1 (b) SPSW3 (c) SPSW5

Fig. 8 Finite element models and buckling mode shapes of SPSWs

Table IV provides the ratios of buckling loads of plates with simple (P_{cr-SS}) and clamped (P_{cr-Cl}) support conditions to those of web plates in SPSW models ($P_{cr-SPSW}$). Comparison of the $P_{cr-SS}/P_{cr-SPSW}$ and $P_{cr-Cl}/P_{cr-SPSW}$ values indicates that the support conditions of infill plates in SPSWs are very close to the clamped support condition.

The limiting thicknesses of web plates in SPSW models are determined through two different approaches, and these results are compared with theoretical predictions for clamped support condition. In the first approach, the exact limiting web-plate thicknesses ($t_{p-SPSW-exact}$) are obtained numerically through an iterative process to reach a concurrent geometrical-material bifurcation condition where $P_y / P_{cr} = 1.0$. In the second approach, a linear interpolation equation, i.e. $t_{p-SS} - \left[(t_{p-SS} - t_{p-Cl}) \times (P_{cr-SPSW} - P_{cr-SS}) / (P_{cr-Cl} - P_{cr-SS})\right]$, is used for predicting the limiting thicknesses of infill plates ($t_{p-SPSW-equation}$). In this equation, t_{p-SS} and t_{p-Cl} are the respective limiting plate thicknesses determined for simple and clamped support conditions, and also P_{cr-SS} and P_{cr-Cl} are the respective theoretically-determined critical buckling loads for simple and clamped support conditions. $P_{cr-SPSW}$ is the critical buckling load of SPSW model obtained from linear eigenbuckling analysis. The values of the limiting plate thicknesses determined through the theoretical and numerical approaches are tabulated in Table V. From the table, agreement between t_{p-Cl}, $t_{p-SPSW-exact}$ and $t_{p-SPSW-equation}$ values is quite satisfactory. It is found that the interpolation equation yields reliable predictions for the limiting plate thickness as well; however, it is noted that application of this equation requires the numerical determination of the SPSW elastic buckling load. Theoretical predictions by considering the clamped support condition, on the other hand, are found to be quite close to the exact values as well. The accuracy of these predictions is further verified by the results obtained from nonlinear finite element analyses and illustrated in Fig. 9.

TABLE IV
BUCKLING LOAD RATIOS OF PLATES WITH DIFFERENT SUPPORT CONDITIONS

Plate $l \times h \times t_p$ (mm)	SPSW model	$P_{cr-SS} / P_{cr-SPSW}$	$P_{cr-Cl} / P_{cr-SPSW}$
2000×3000×10.6	SPSW1	0.53	0.85
3000×3000×9.3	SPSW2	0.59	0.91
3000×3000×14.0	SPSW3	0.60	0.93
3000×3000×18.7	SPSW4	0.60	0.93
4500×3000×15.8	SPSW5	0.67	1.08

TABLE V
LIMITING THICKNESSES OF PLATES DETERMINED THROUGH DIFFERENT APPROACHES

$l \times h$ (mm)	t_{p-SS} (mm)	t_{p-Cl} (mm)	$t_{p-SPSW-exact}$ (mm)	$t_{p-SPSW-equation}$ (mm)
2000×3000	13.4	10.6	10.3	9.3
3000×3000	17.5	14.0	13.5	13.1
3000×3000	17.5	14.0	13.5	13.2
3000×3000	17.5	14.0	13.5	13.3
4500×3000	20.1	15.8	16.0	16.6

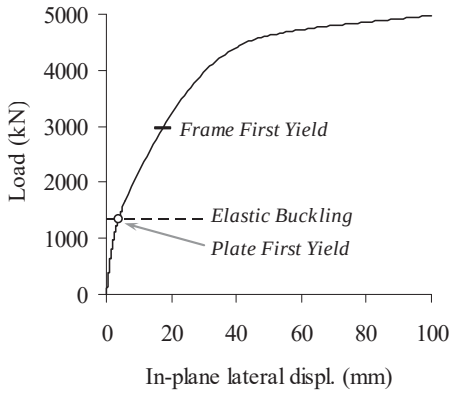

(a) SPSW1, $t_{p-SPSW-exact}$ = 10.3 mm

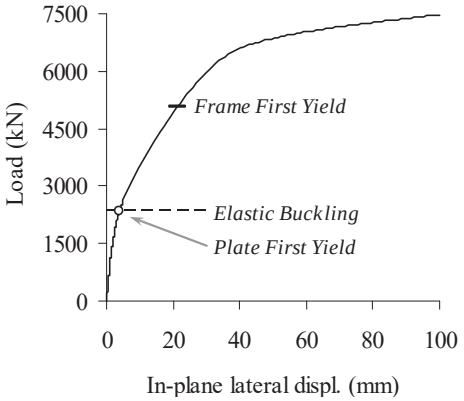

(b) SPSW3, $t_{p-SPSW-exact}$ = 13.5 mm

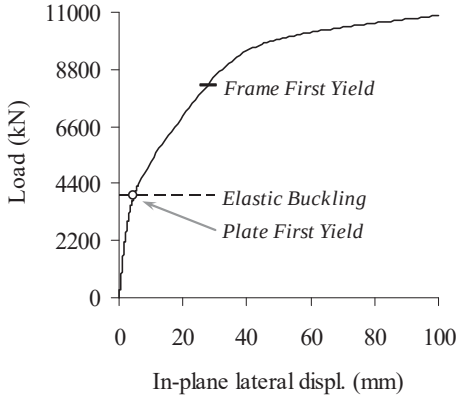

(c) SPSW5, $t_{p-SPSW-exact}$ = 16.0 mm

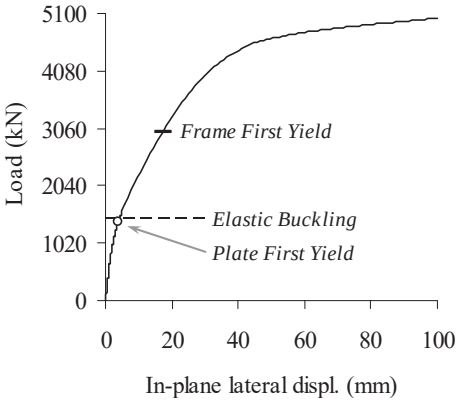

(d) SPSW1, t_{p-Cl} = 10.6 mm

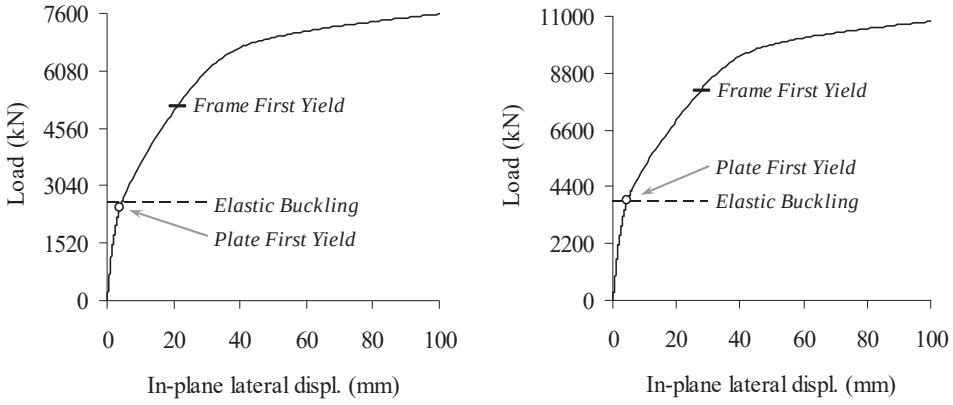

(e) SPSW3, $t_{p\text{-}Cl} = 14.0$ mm (f) SPSW5, $t_{p\text{-}Cl} = 15.8$ mm

Fig. 9 Buckling and yielding behaviors of SPSW1, SPSW3, and SPSW5 models

By comparing the results in Figs. 9 (a) and (d), (b) and (e), and (c) and (f), it is found that theoretical predictions of the limiting plate thickness considering clamped support condition result in simultaneous buckling and yielding of infill plates in all three cases. By considering the simplicity of this theoretical approach as discussed in Section II, and also based on the findings of this study, it may be concluded that limiting thicknesses of infill plates in SPSW systems can be fairly accurately predicted by considering the clamped support condition, given that the boundary frame members are designed properly.

VII. Conclusion

In this paper, the buckling and yielding behaviors of LYP steel plates with various support and loading conditions were investigated through finite element analysis. The limiting thicknesses of simply supported and clamped plates under pure shear and combined shear and compression, corresponding to concurrent geometrical-material bifurcation were determined through theoretical approaches, and subsequently verified via detailed numerical simulations.

It was shown that use of LYP steel considerably reduces the limiting plate thickness. Moreover, it was found that higher plate length-to-height ratio unfavorably results in larger limiting plate thickness. Moreover, results of this study also demonstrated that limiting thicknesses of infill plates in SPSWs can be easily and fairly accurately determined in practice by considering the clamped support condition.

Considering the early yielding and ductility of LYP steel infill plates in SPSWs, accurate determination and consideration of the limiting plate thickness as an important design criterion can result in design of high-performing SPSW systems with desirable structural and seismic characteristics. It is noted that this is made economically possible in the light of use of LYP steel.

References

[1] Alinia M.M., Gheitasi A. and Erfani S. (2009). "Plastic shear buckling of unstiffened stocky plates", Journal of Constructional Steel Research, 65(8-9) 1631-1643.
[2] Gheitasi A. and Alinia M.M. (2010). "Slenderness classification of unstiffened metal plates under shear loading", Thin-Walled Structures, 48(7), 508-518.
[3] Chen S.J. and Jhang C. (2006). "Cyclic behavior of low yield point steel shear walls", Thin-Walled Structures, 44(7), 730-738.
[4] Chen S.J. and Jhang C. (2011). "Experimental study of low-yield-point steel plate shear wall under in-plane load", Journal of Constructional Steel Research, 67(6), 977-985.
[5] Timoshenko S.P. and Gere J.M. (1961). Theory of Elastic Stability. McGraw-Hill, New York.
[6] Chen Y.Z., Lee Y.Y., Li Q.S. and Guo Y.J. (2009). "Concise formula for the critical buckling stresses of an elastic plate under biaxial compression and shear", Journal of Constructional Steel Research, 65(7), 1507-1510.
[7] ANSYS 11.0 (2007). ANSYS 11.0 documentation, ANSYS Inc.
[8] Zoruba S. and Liddy W. (2007). "Steelwise: Structural steel materials update", Modern Steel Construction Magazine, AISC, March issue.
[9] Yamaguchi T., Nakata Y., Takeuchi T., Ikebe T., Nagao T., Minami A. and Suzuki T. (1998). Seismic Control Devices Using Low-Yield-Point Steel. Nippon Steel Technical Report No. 77, 78 July, 65-72.
[10] AISC 341-10 (2010). Seismic Provisions for Structural Steel Buildings. American Institute of Steel Construction, Chicago, IL.